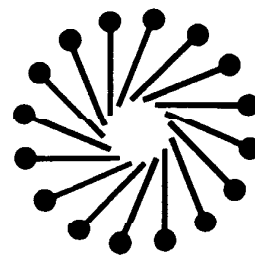


# **TENSIDE** **SURFACTANTS** **DETERGENTS**

Zeitschrift für Physik, Chemie und Anwendung grenzflächenaktiver Stoffe  
Journal for Theory, Technology and Application of Surfactants



34. Jahrgang

Alle Rechte, auch die des Nachdrucks,  
der photomechanischen Wiedergabe  
dieses Autorenfortdrucks  
und der Übersetzung,  
behält sich der Verlag vor.

Carl Hanser Verlag  
Kolbergerstraße 22  
81679 München  
Tel.: (089)99830-117  
Fax: (089)99830 624

# AUTOREN

# FORTDRUCKE

# 1997



R. Miller\*, Berlin/Germany, V. B. Fainerman, Donetsk/Ukraine, K.-H. Schano, Berlin/Germany, A. Hofmann and W. Heyer, Lauda-Königshofen/Germany

# Dynamic surface tension determination using an automated bubble pressure tensiometer

*A newly designed fully automated maximum bubble pressure tensiometer has many advantages compared to known instruments developed so far. The most striking feature is the possibility to determine the bubble dead time and to calculate the efficient surface age of a bubble. The state of the art of the theory for describing adsorption processes at the surface of a growing bubble is discussed and useful approximate solutions are given and applied to example experiments. The temperature and viscosity dependence of the adsorption kinetics of a model surfactant, Triton X-100, are discussed in terms of a diffusion controlled adsorption model. Finally, as an example, measurements of human blood and urine samples are presented in order to show the sensitivity of dynamic surface tensions to changes in the composition of such complex liquids. Measurements of river water samples show an additional field of application in water treatment control.*

*Ein vor kurzem entwickeltes vollautomatisches Blasendrucktensiometer hat viele Vorteile gegenüber bisher bekannten Geräten. Ein herausragender Vorteil ist die Möglichkeit, die Totzeit bei der Blasenbildung und das effektive Oberflächenalter einer Blase zu bestimmen. Der Stand der Theorie zur Beschreibung von Adsorptionsprozessen an der Oberfläche einer wachsenden Blase wird erörtert, es werden nützliche Näherungslösungen angegeben und an experimentellen Beispielen verifiziert. Die Abhängigkeit der Adsorptionskinetik eines Modelltensids, Triton X-100, von Temperatur und Viskosität wird auf der Grundlage des Modells der diffusionskontrollierten Adsorption diskutiert. Als Beispiele werden Meßergebnisse von Proben von menschlichem Blut und Urin angeführt, um zu demonstrieren, wie empfindlich die dynamische Oberflächenspannung auf Änderungen in der Zusammensetzung solcher komplexen Flüssigkeiten reagiert. Messungen an Flußwasser ergeben, daß in der Überwachung von Wasseraufbereitungsanlagen eine weitere Applikationsmöglichkeit liegt.*

## 1 Introduction

The maximum bubble pressure technique is one of the classical methods in surface science. Due to the fast development of new technique and the great interest in recent years in experiments at very short adsorption times, commercial set-ups were built to make the method available for a large number of researchers [1]. Reh binder [2, 3] was the first who used this technique for the determination of the dynamic surface tension of surfactant solutions. Further developments were described by several authors [4–11].

The first theoretical background was established by Austin et al. [8]. He defined the time interval between two subsequent bubbles as the surface lifetime and the so-called "dead time",  $\tau_d$ , which is the time required to detach after the bubble has reached a hemispherical shape. Kloubek [12–14] made a remarkable contribution for the further development of this method by deriving a simple experimental procedure for the determination of the dead time and giving an estimate of the effective bubble surface age [14].

The use of electric pressure sensors for the determination of pressure and bubble formation frequency [9, 15–19] simplified the determination procedure and many original designs for dynamic surface tension determinations by the maximum bubble pressure method have been presented [18, 20–27].

The purpose of the present paper is to present a new designed automated bubble pressure instrument and to compare its principles with other typical experimental set-ups. Advantages and disadvantages are discussed and experimental examples are given to show the broad range of applications.

## 2 Maximum bubble pressure technique

The design of a maximum bubble pressure method for high bubble formation frequencies must address three main problems: the determination of the bubble pressure and the bubble formation frequency and the estimation of surface lifetime and effective surface age.

The first problem can be solved easily if the system volume, which is connected with the bubble, is large enough compared to the volume of the bubble separating from the capillary. In this case the system pressure is equal to the maximum bubble pressure. The use of an electric pressure transducer for measuring the bubble formation frequency presumes however that pressure oscillations in the measuring system are distinct enough. This condition is fulfilled in systems with comparatively small volumes only. In Fig. 1 these two principally different set-ups are shown with their main components. Part b of the schematic representation corresponds to the set-up which is referred to in this paper, the MPT2 from LAUDA.

Instruments based on the principle (a) simply determine the time dependence of the pressure at sensor (1) at a certain

\* Author to whom correspondence should be sent: Max-Planck-Institut für Kolloid- und Grenzflächenforschung, Rudower Chaussee 5, D-12489 Berlin-Adlershof, Germany

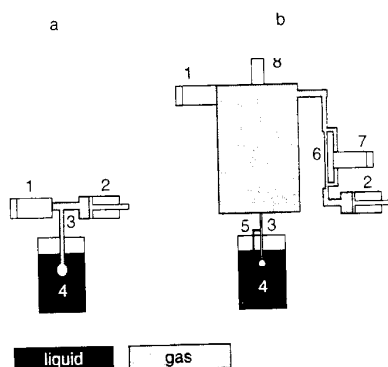


Fig. 1. Schematic design of usual bubble pressure instruments (a) and the automated bubble pressure tensiometer (b); 1 - pressure sensor, 2 - gas supply (pump or compressor), 3 - capillary, 4 - solution to be studied, 5 - "nose" to control a constant bubble size, 6 - flow rate capillary, 7 - pressure sensor for determining the gas flow rate, 8 - microphone

air flow produced by the gas supply (2). The instrument (b) works with constant gas flow produced by a pump (2) and controlled by a second pressure sensor (7) and a flow capillary (6). The pressure  $P$  of the system is determined with the pressure sensor (1) at different constant gas flow rates  $L$ . For more details see for example *Fainerman et al.* [28-30].

As shown by *Mysels* [19], the determination of maximum bubble pressure values in systems with a small volume can be erroneous. The pressure changes in these two types of bubble pressure instruments are shown schematically in Fig. 2.

Due to the large ratio of bubble to system volume (of the order of 1:100,000) the pressure in the system (sensor 1) remains constant at any time, if the air flow rate is kept constant. Only the pressure in the bubble itself changes with its size. In contrast to instruments with small system volume, the pressure in the system (at the sensor 1) and in the bubble changes with the bubble size. Because of the distance between the bubble and the sensor a change in the pressure amplitude as well as a phase shift result.

The advantage of instruments with small system volumes is the possibility of direct bubble frequency determination, while set-ups with large system volumes need an additional indicator. The presented instrument uses two separate systems, an electric and an acoustic sensor (part 8 in Fig. 1) for the exact determination of the bubble frequency.

The third problem to be solved in a bubble pressure tensiometer is the determination of the lifetime of a bubble,

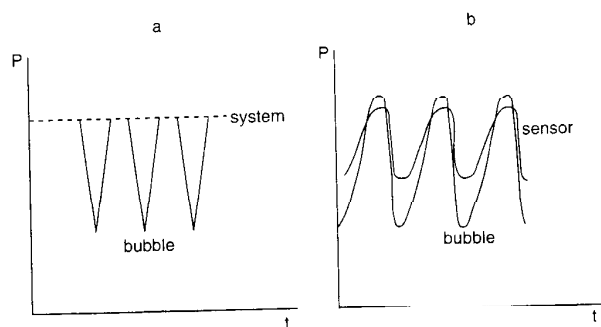


Fig. 2. Principal course of the pressure  $P$  as a function of time for different instruments; a - MPTI, b-usually designed bubble pressure instruments

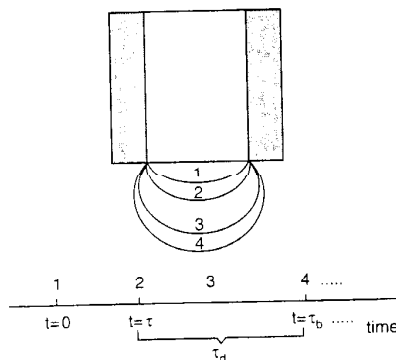


Fig. 3. Different stages of bubble formation and definition of characteristic bubble times; 1 - initial bubble size, 2 - hemispherical size (maximum pressure), 3 - intermediate state, 4 - final size before detachment

the period between its beginning until its hemispherical size. Fig. 3 demonstrates the different stages of bubble formation. The time interval between the hemispherical size and the final size in the moment of bubble detachment is called the dead time  $\tau_d$ .

To separate the surface lifetime from the total time interval between subsequent bubbles an approximation of the dead time according to geometric parameters of capillary and bubble volume was derived by *Fainerman* and *Lylyk* [28] and *Fainerman* [29]. A substantial improvement for the exact determination of surface lifetime and its calculation was carried out by *Fainerman* [30] who defined a critical point in the experimental curve "Pressure-gas flow rate". A principle curve  $P$  as a function of air flow rate is given in Fig. 4. This point corresponds to a change in the flow regime from individual bubble formation to a gas jet regime with increasing flow rate  $L$ . At high air flow rates the time a bubble needs to separate from the residual gas is too large to form individual bubbles. At lower flow rates this time is sufficiently long to form single bubbles. The two regimes are schematically shown in Fig. 5 as a function of air flow rate. After a certain gas flow rate has been reached, single bubbles are formed.

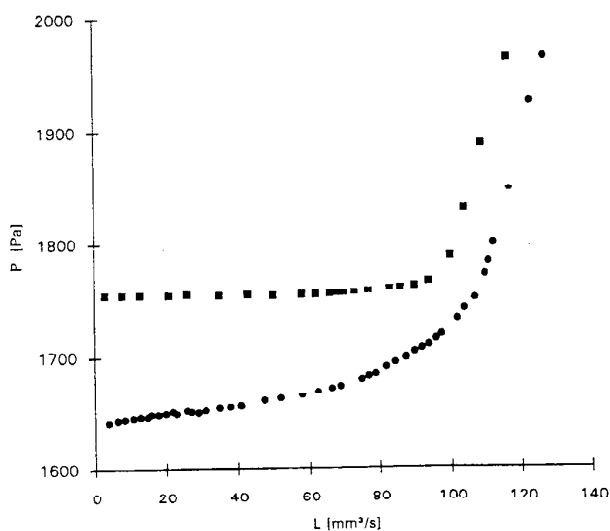


Fig. 4. Dependence of the system pressure  $P$  on the gas flow rate  $L$  for water (■) and a surfactant solution (●)

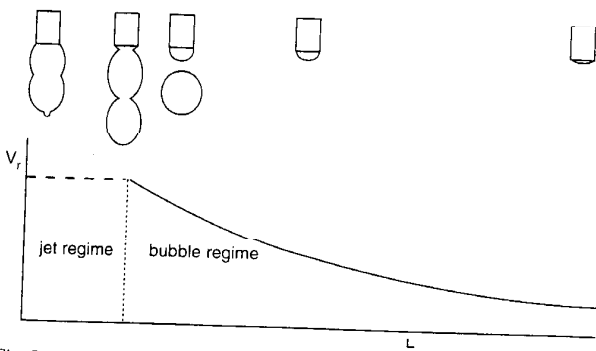


Fig. 5. Different states of gas flow at the tip of a capillary, transition from a gas jet to a single bubble regime at a definite gas flow rate

The volume  $V$  of the residual bubbles, after a bubble detached is decreasing with lower flow rates  $L$ . The value of  $\tau_d$ , equivalent to the time interval necessary to form a bubble of the radius  $R$ , can be calculated using Poiseuille's law, as long as the condition  $p = \text{const}$  holds in the system [29–31]

$$\tau_d = \frac{\tau_b L}{K P} \left( 1 + \frac{3 r_{\text{cap}}}{2 R} \right), \quad (1)$$

where  $K = \tau^4/81 \eta$  is the Poiseuille law constant (for a non-immersed capillary Eq. (1) reads  $L = K p$ ),  $\eta$  is the gas viscosity,  $l$  is the length and  $r_{\text{cap}}$  the radius of the tip of the capillary. The calculation of the dead time  $\tau_d$  can be simplified when taking into account the existence of the two gas flow regimes for the gas flow leaving the capillary, according to Fig. 4. Exactly at the transition between the two regimes  $\tau_d = 0$  and hence  $\tau_b = \tau_d$ .

On the right hand side of the critical point the dependence of  $p$  on  $L$  is linear in accordance with Poiseuille's law. The existence of the electrode placed opposite the capillary controls the dimension of bubbles. Under this condition the bubble radius, and consequently the bubble volume, is constant at any given  $L$  inside the bubble flow regime. Instead of Eq. (1) the following simplified equation therefore results to determine  $\tau_d$  [29],

$$\tau_d = \tau_b \frac{L P_c}{L_c P}, \quad (2)$$

where  $L_c$  and  $P_c$  are related to the critical point, and  $L$  and  $P$  are the actual values of the dependence left from the critical point. This derivation for the calculation of the dead time is based on the assumption of a constant bubble volume, which is arranged in the MPT2 by a "nose", bringing the growing

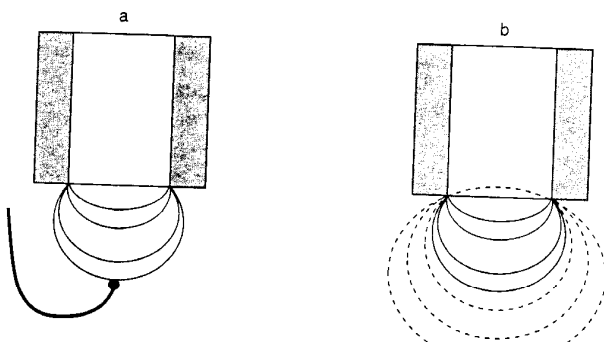


Fig. 6. Bubble formation in the presence of a "nose" located opposite to the capillary tip (a) and in absence of it (b)

bubbles out of symmetry after they have reached a definite bubble size (corresponding to a bubble radius  $R$ ). Without such a nose, the size of a detaching bubble can scatter considerably. This fact is demonstrated in Fig. 6. Consequently, the surface lifetime can be calculated by formula

$$\tau = \tau_b - \tau_d = \tau_b \left( 1 - \frac{L P_c}{L_c P} \right). \quad (3)$$

As one can see, Eq. (3) involves only experimentally available values. The critical point in the dependence  $p$  on  $L$  can easily be located. In the software the location is automatically calculated by an algorithm based on the Poiseuille law.

The MP12 provides two possible measuring cells, one for the use with both bubble frequency sensors and the other for use with the acoustic sensor only (Fig. 7). The second type

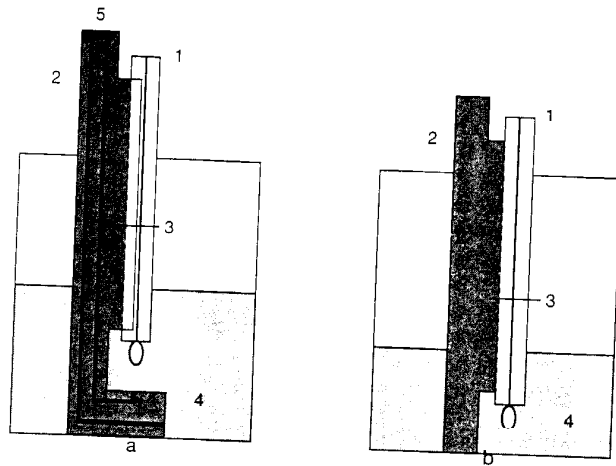


Fig. 7. Measuring cells of the MPT1; 1 – capillary, 2 – capillary holder, 3 – ring to fix the position of the capillary in the holder precisely, 4 – liquid, 5 – electrical sensor

(b) has the advantage that only a very little amount of measuring liquid is needed, so that even biological and medical liquids, such as blood, can be easily studied [32].

The calculation of the so-called effective age of the surface (effective adsorption time) from the bubble surface lifetime was discussed by many authors: Joos and Rillaerts [33], Garrett and Ward [34], Fainerman [30], Fainerman et al. [35]. The derivation of the relative surface deformation rate is based on the condition  $P = \text{const}$ . To calculate the effective surface age (adsorption time) the following equation results [30, 35]:

$$\tau_a = \frac{\tau}{2 \xi + 1} \quad (4)$$

where  $\xi = \frac{2 \sin \varphi_0}{2 + \sin \varphi_0}$  is the mean relative deformation rate of the bubble surface in the first stage of its growth, and  $\varphi_0 = \arccos(\gamma/\gamma_0)$ . For values of  $\gamma$  not too close to  $\gamma_0$  (for example, for aqueous solutions below 60 mN/m),  $\xi$  is approximately equal to 0.5, and consequently  $\tau_a = \tau/2$ , at very low surface tension changes the relation becomes  $\tau_a = 3\tau/7$ , identical with the situation of growing drops. Most of the instruments, based on the principle of maximum bubble pressure, do not allow the effective surface age to be calculated because the conditions during the bubble formation are unknown.

A more precise analysis of the effective surface age would be possible if the recently developed theory of radially grow-

ing spherical drops and bubbles is applied [36, 37]. The main equation

$$\frac{d\Gamma}{dt} = -(\Gamma(t))^2 \sqrt{\frac{D}{\pi}} \int_0^t \frac{\left(\frac{dc(0,t)}{dt}\right)_{t_0}}{\int_0^t (\Gamma(\xi)^4 d\xi)^{1/2}} dt_0 - \Gamma \frac{d \ln A}{dt} \quad (5)$$

has to be completed by the corresponding initial conditions and the correct  $R(t)$ -function ( $R$  – radius of the bubble,  $\Gamma$  – surface concentration,  $c(0, t)$  – bulk concentration adjacent to the interface,  $D$  – diffusion coefficient,  $A$  – surface area of the bubble). This numerical work is under way.

The surface tension value in the maximum bubble pressure method is calculated via the Laplace equation. For the instrument under discussion, the capillary radius is small and the bubble shape is thus assumed to be spherical. Hence, the deviation of the bubble shape from a spherical one can be neglected and needs no correction so that the following equation results,

$$p = \frac{2\gamma}{r_{\text{cap}}} + \rho g h + \Delta p \quad (6)$$

where  $\rho$  is the density of the liquid,  $g$  is the acceleration of gravity,  $h$  is the depth the capillary is immersed into the liquid, and  $\Delta p$  is a correction value to allow for hydrodynamic effects.  $\Delta p < 0$  results in a correction of  $\Delta\gamma = \gamma_{\text{app}} - \gamma_{\text{corr}} > 0$  (indices “app” and “corr” stand for apparent and corrected surface tensions, respectively) which can be estimated according to the following relation,

$$\Delta\gamma = \frac{3}{2} \frac{\eta r}{\tau} \quad (7)$$

Recent experimental studies [38] corroborated qualitatively the validity of Eq. (7): the value increases with increasing liquid viscosity  $\eta$ , increasing capillary radius  $r_{\text{cap}}$  and decreasing surface lifetime  $\tau$ . *Kao et al.* [39] and *Edwards et al.* [40] made an analysis of surface and bulk rheological effects on the growth and rising of gas bubbles in a bubble pressure experiment and found a term to calculate the bulk viscosity influence comparable with Eq. (7). For aqueous surfactant solutions this effect should be negligible, which is in full agreement with the results of *Fainerman et al.* [38]. At higher viscosities, this bulk viscosity effect has a remarkable effect on the bubble formation and has to be allowed for, also in the experiments to study dilational viscosity proposed by *Kao et al.* [39].

The maximum bubble pressure method, realised as the set-up MPT2, allows measurements in a time interval from 1–2 ms up to several seconds and in the stopped flow regime up to even 100 seconds. At present, it is the only commercial apparatus which produces adsorption data in the millisecond range. Otherwise data in this time interval can otherwise be obtained only from laboratory set-ups of the oscillating jet, inclined plate or other, even more sophisticated methods. The accuracy of surface tension measurements in the time interval of milliseconds is about  $\pm 0.5$  mN/m, at effective surface ages  $\tau_a > 0.01$  s the accuracy is  $\pm 0.1$  mN/m. Experimental data obtained by this technique and comparisons with other measuring techniques are given below. Due to its time window, the maximum bubble pressure method even provides the possibility to study the effect of micelle kinetics on the adsorption process of surfactants and thus is an experimental source for information about rate constants of micelle formation or dissolution processes [41, 42].

Data at longer bubble time are obtained with a stopped flow regime. This is achieved by switching off the gas flow

closing a magnetic valve, after a sufficiently low bubble frequency has been reached. Due to the further lowering of the surface tension with longer adsorption time (longer bubble time) the internal pressure in the system  $V_s$ , having a volume of about 50 cm<sup>3</sup>, allows to produce further bubbles. The volume of each of the bubbles  $V_b$  amounts to 2 to 5 mm<sup>3</sup>, depending on the geometry of the measuring cell. The pressure inside the system  $P_s$  (about the atmospheric pressure of 10<sup>5</sup> Pa) decreases with the detachment of one bubble by the value  $\Delta P = P_s V_b / V_s \approx 4 \div 10$  Pa. The detachment of each bubble corresponds to a surface tension decrease of  $\delta\gamma = \Delta P r_{\text{cap}} / 2$ . The measured pressure in the system and the time interval between two bubbles lead to the time dependence of surface tension at times  $t > 2s$ . The modified programme of the MPT2 allows a fully automatic run of the standard procedure as well as the stopped flow regime, leading to dynamic surface tensions in the respective time intervals.

### 3 Description of the adsorption process at the surface of a growing bubble

The kinetics of the adsorption process taking place at the surface of a growing bubble is important for the interpretation of data from maximum bubble pressure experiments. The same problem has to be solved in any other experiment based on growing drops or bubbles, such as bubble and drop pressure measurements with continuous, harmonic or transient area changes [for example 36, 37, 43–48].

*Ilkovic* [49, 50] was the first who discussed the adsorption at a growing drop surface. The same situation is correct for a growing bubble. A complete diffusion-controlled adsorption model, considering the radial flow inside a growing drop, was derived by *Pearson and Whittaker* [51]. The bubble growth is connected with a flow outside the bubble and a surface area enlargement. The flow outside the bubble can be assumed to be radial. Although the area stretching is not totally isotropic no significant deviations are expected and, therefore, no flow normal to the interface is initiated. Nevertheless, the stretching of the interface simultaneously leads to a stretching of the adjacent liquid layers. As a consequence, the concentration profile caused by diffusion is compressed. As a consequence, two processes overlap and are directed opposite to each other: diffusion layer compression due to the enlargement of the bubble, and diffusion layer dilation due to the growth of the bubble area and dilation of the adsorption layer coverage. Both counteracting processes have been taken into consideration in current theories.

In analogy to the *Ward and Tordai* equation [52] the following non-linear integral equation was derived on the basis of the above given assumptions [53]:

$$\Gamma(t) = 2c_0 \sqrt{\frac{3Dt}{\pi}} - \sqrt{\frac{D}{\pi}} t^{-2/3} \int_0^{3/7} \frac{c\left(0, \frac{7}{3} \lambda^{3/7}\right)}{\left(\frac{3}{7} t^{7/3} - \lambda\right)^{1/2}} d\lambda \quad (8)$$

Eq. (8) can be used to describe the adsorption process at the surface of growing drops and bubbles as long as their volume increases linearly. This is true for drops with a linear liquid dosing system and for bubbles within the time interval up to the hemispherical size. The analysis of this rather complex equation showed that the rate of adsorption at the surface of a growing drop or bubble with linear volume increase changes from 3/7 to about 1/4 of that at a surface with constant area. This result is supported by experimental findings

with the drop volume method [13, 14, 54–56] and also by an approximate solution first discussed by *Delahay* and *Trachtenberg* [57] and *Delahay* and *Fike* [58]:

$$l'(t) = 2c_0\sqrt{\frac{3D}{7\pi}}t \quad (9)$$

Different flow patterns, also a turbulent flow, were considered by *Fainerman* [59] for the discussion of kinetic data obtained from dynamic drop volume experiments.

A more advanced theory of the adsorption process at growing spherical surfaces was made by *MacLeod* and *Radke* [37]. In contrast to the theory discussed above they do not assume a point source at the beginning of the process but a finite drop size. On the basis of an arbitrary dependence  $R(t)$  a theory of diffusion – as well as kinetically-controlled adsorption was then derived. The result is given by the equation

$$\frac{d\Gamma}{dt} = -(R(t))^2 \sqrt{\frac{D}{\pi}} \int_0^t \left( \frac{dc(0,t)}{dt} \right)_{t_0} dt_0 - \Gamma \frac{d \ln A}{dt} \quad (10)$$

Although this is a very complex equation, it allows to take into consideration any function of  $R(t)$ , and consequently  $A(t)$ , resulting from experiments with growing drops or bubbles. In combination with an adsorption isotherm (diffusion-controlled case) or a transfer mechanism (mixed diffusion-kinetic-controlled model) it describes the adsorption process at a growing drop or bubble. Eq. (10) can be applied in its present form only via numerical calculations and an algorithm is given by *MacLeod* and *Radke* [37]. A detailed analysis of bubble pressure experiments does not exist so far, but it is possible on the basis of Eq. (10).

The pure kinetic-controlled adsorption process can of course be modelled by the simple combination of any transfer mechanism and the change of adsorption with time under the condition of surface area changes. Such models have been derived by *Miller* [53]:

$$\frac{d(\Gamma A)}{dt} = A(t)(j_{ad} - j_{des}) \quad (11)$$

Here,  $j_{ad}$  and  $j_{des}$  are the adsorption and desorption fluxes, respectively. Considering a Langmuir mechanism, Eq. (11) takes the final form:

$$\frac{d\Gamma}{dt} = k_{ad} \left( 1 - \frac{\Gamma}{\Gamma_{\infty}} \right) - k_{des} \frac{\Gamma}{\Gamma_{\infty}} - \Gamma \frac{d \ln A}{dt} \quad (12)$$

Dependent on the form of  $A(t)$ , Eq. (12) can be solved analytically or has to be approximated by a numerical algorithm.

Recently, approximate solutions were derived which are very useful for fast data interpretation. For example the dynamic surface tension  $\gamma(t)$  of a single surfactant solution at

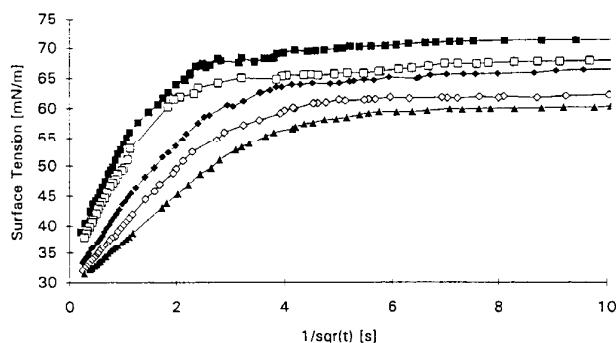


Fig. 8. Dynamic surface tension of a  $1.55 \times 10^{-7} \text{ mol/cm}^3$  Triton X-100 solution at different temperatures in a  $\gamma(1/\sqrt{t})$ -plot: 30°C (■), 40°C (□), 50°C (◆), 60°C (◇), 70°C (▲)

long adsorption time is well described by the characteristic slope given by *Fainerman* et al. [60].

$$\left[ \frac{d\gamma}{dt^{-1/2}} \right]_{t \rightarrow \infty} = \frac{R T \Gamma_0^2}{c_0} \sqrt{\frac{\mu}{4D}} \quad (13)$$

where  $\Gamma_0$  is the equilibrium adsorption at concentration  $c_0$ ,  $R$  and  $T$  are the gas law constant and absolute temperature, respectively.

In the range of small adsorption time the relation

$$\left[ \frac{d\gamma}{dt^{-1/2}} \right]_{t \rightarrow 0} = -2 R T c_0 \sqrt{\frac{D}{\pi}} \quad (14)$$

results, which allows to determine the diffusion coefficient from the initial slope of the corresponding plot.

#### 4 Experimental examples

The described maximum bubble pressure tensiometer is applicable to many different liquids. To prove its correct operation, simultaneous measurements of dynamic surface tension of the same surfactant solution with the MPT2 and different other techniques were carried out: oscillating jet and inclined plate [61, 62] and drop volume method [63]. The results are of good accuracy and reproducibility and always within the limit of accuracy of the used experimental techniques.

To demonstrate the wide variety of application, some examples are given here. Fig. 8 presents the dynamic surface tension of a Triton X-100 solution at different temperatures in a  $\gamma(1/\sqrt{t})$  plot. Tab. 1 summarises some important parameters of these measurements. The values of  $\gamma_{H_2O}$  are obtained from extrapolations using Eq. (14). The obtained values are in rather good agreement with data from the literature [64]. The  $\gamma_{\infty}$ -values are obtained from extrapolations according to Eq. (13).

Table 1. Characteristic data for a  $1.55 \times 10^{-7} \text{ mol/cm}^3$  Triton X-100 solution at different temperatures

Temperature [°C]	$\gamma_{H_2O}$ [mN/m]	$\gamma_{H_2O}$ [mN/m] after ref. [64]	$\gamma_{\infty}$ [mN/m]	$\left[ \frac{d\gamma}{dt^{-1/2}} \right]_{t \rightarrow \infty} \left[ \frac{\text{mN} \sqrt{\text{s}}}{\text{m}} \right]$
30	71.2	71.4	35.5	17
40	69.5	69.4	34	16
50	68.0	67.4	30.8	13
60	65.6	-	29.8	10
70	64.3	-	29	8

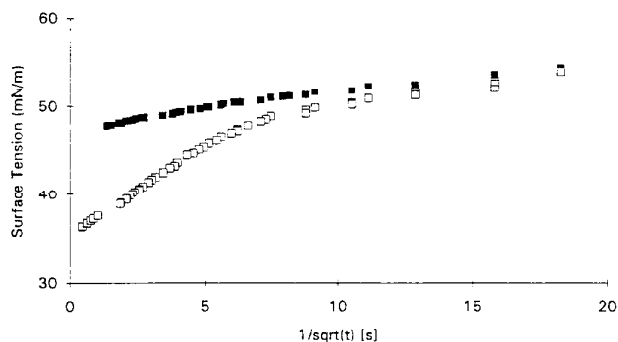


Fig. 9. Dynamic surface tension  $\gamma$  as a function of  $(1/\sqrt{t})$  of mixed surfactant solutions;  $5 \times 10^{-6} \text{ mol/cm}^3$  SDS without (■) and mixed with  $2.82 \times 10^{-7} \text{ mol/cm}^3$  Triton X-114 (□)

As shown in [60] for example, the slope of these curves (Eq. 13) provides information about the diffusion coefficient assumed a diffusion-controlled adsorption model is applied.

The values of the slope  $\left[ \frac{d\gamma}{dt^{-1/2}} \right]_{t \rightarrow \infty}$  are also included in Tab.

1. To calculate the diffusion coefficient from these values, exact data of the surface concentration at different temperatures are needed. Those values are not available so far for the large temperature interval, so that the slopes  $S(T)$  can only be compared with each other. According to Einstein's equation the diffusion coefficient changes proportional to the total temperature. The change of the slope  $S$  with temperature to lower values indicates that the equilibrium surface concentration decreases significantly with increasing temperature, which is in accordance with the common idea of surfactant adsorption.

The dynamic surface tension of an SDS solution in absence and presence of a second surfactant Triton X-100 is given in Fig. 9. The SDS alone has reached its adsorption equilibrium already at rather short adsorption times. The slope of the  $\gamma(1/\sqrt{t})$ -curve for the mixture is therefore mainly determined by the Triton X-100 molecules [65].

In a recent paper the dynamic surface tensions of sodium tetradecyl sulphate in highly viscous water/glycol mixtures were studied. As the result the adsorption kinetics of the surfactant was discussed in terms of diffusion transport of the surface active molecules in the viscous bulk. The studies proved that the bubble pressure tensiometer yields reliable surface tension data even for highly viscous solutions.

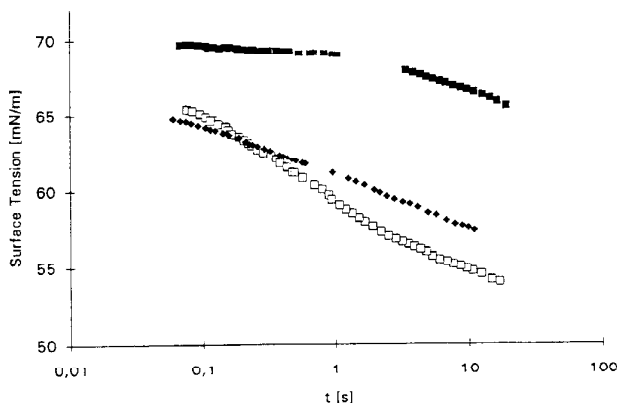


Fig. 10. Dynamic surface tension of urine samples of 3 patients (■) – healthy person (□♦) – with different nephrological diseases

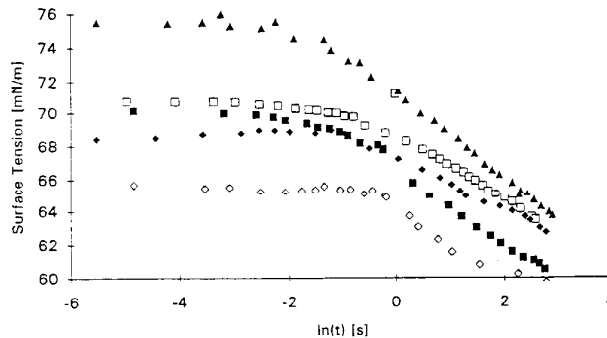


Fig. 11. Dynamic surface tension of blood samples of 5 patients with chronic pyelonephritis

As a final example we want to show the application of the maximum bubble pressure tensiometer in medicine and water purity control. The dynamic surface tensions of urine samples show interesting features which can be used as index to characterise the state of different diseases [32]. In Fig. 10 the dynamic surface tension of urine samples of three patients is displayed. Person 1 does not show any biochemical data beyond the norm values (healthy) while persons 2 and 3 suffer from different nephrological diseases. The dynamic surface tensions of blood samples of different patients (chronical pyelonephritis) are shown in Fig. 11. The curves demonstrate that the values of  $\left( d\gamma/d\frac{1}{\sqrt{t}} \right)_{t \rightarrow \infty}$  are very similar but are significantly different from those of healthy people. For one and the same medical diagnosis a good correlation between this dynamic surface tension parameter and biochemical data of blood was found: higher plateau values  $\gamma_{t \rightarrow 0}$  correlate with higher contents of immunoglobulins and lower amounts of albumins.

A broader discussion of the sensitivity of dynamic surface tension to the composition of such complex biological liquids like the human urine and the possibility of using specific surface tension values as index in medical diagnosis was given for the first time by Fainerman et al. [32].

Another field of application of the maximum bubble pressure method can be seen in the control of industrial waste water or drinking water from water treatment plants with respect to traces of surface active contaminations. The results of dynamic surface tension measurements of distilled water and a water sample from the river Kalmius (sample was taken from the river at a place located within Donetsk, Ukraine) are shown in Fig. 12 as  $\gamma(\sqrt{t})$ -plots. These data are

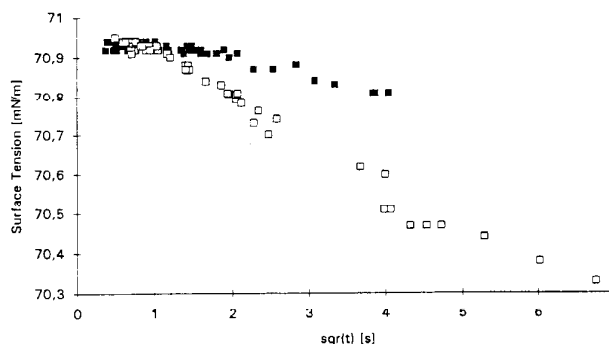


Fig. 12. Dynamic surface tension of distilled water (■) and river water (Kalmius) (□)

obtained by using the stopped flow procedure of the MPT2. When we interpret these data using Eq. (14), we can estimate the concentration of surface active compounds in the water from the slope of  $(d\gamma/d\sqrt{t})_{t \rightarrow 0}$ . The water sample from the river Kalmius yields  $c_0 = 1.5 \times 10^{-9}$  mol/cm<sup>3</sup>, which corresponds to an amount of 0.45 mg/l assuming an average molecular weight of 300 g/mole. This result is in excellent agreement with data from a chemical analysis of ionic surfactants in the river, where 0.1 to 0.8 mg/l was found.

### Acknowledgements

The work was financially supported by projects of the European Community (HCM ERBCHRXT 930322 and INTAS 93-2463) and the Fonds der Chemischen Industrie (RM 400429). We also would like to thank the MPI for a fellowship for one of us (VBF). The help in solving many technical and software problems by A. Vertlyb and A. Zadov is gratefully acknowledged.

### References

1. Adamson, A.W.: Physical Chemistry of Surfaces, 5th Edition, John Wiley Sons, Inc., New York, 1990.
2. Rehinder, P.A.: Z. Phys. Chem., 111 (1924) 447.
3. Rehinder, P.A.: Biochem. Z., 187 (1927) 19.
4. Sugden, S.: J. Chem. Soc., 125 (1924) 27.
5. Adam, N.K. and Shute, H.L.: Trans. Faraday Soc., 31 (1935) 204.
6. Adam, N.K. and Shute, H.L.: Trans. Faraday Soc., 34 (1938) 758.
7. Kuffner, R.J.: J. Colloid Sci., 16 (1961) 797.
8. Austin, M., Bright, B.B. and Simpson, E.A.: J. Colloid Interface Sci., 23 (1967) 108.
9. Bendure, R.L.: J. Colloid Interface Sci., 35 (1971) 238.
10. Finch, J.A. and Smith, G.W.: J. Colloid Interface Sci., 45 (1973) 81.
11. Krugh, A.M.: Trans. Faraday Soc., 60 (1964) 225.
12. Kloubek, J.: Tenside 5 (1968) 317.
13. Kloubek, J.: J. Colloid Interface Sci., 41 (1972) 1.
14. Kloubek, J.: J. Colloid Interface Sci., 41 (1972) 7.
15. Razouk, R. and Walmsley, D.: J. Colloid Interface Sci., 47 (1974) 515.
16. Miller, T.E. and Meyer, W.C.: American Laboratory, Feb. (1984) 91.
17. Woolfrey, S.G., Banzon, G.M. and Groves, M.J.: J. Colloid Interface Sci., 112 (1986) 583.
18. Hua, X.Y. and Rosen, M.J.: J. Colloid Interface Sci., 124 (1988) 652.
19. Mysels, K.J.: Langmuir, 5(1989) 442.
20. Ramakrishnan, S., Mailliet, K. and Hartland, S.: Proc. Indian Acad. Sci., 83A (1976) 107.
21. Tzykurina, N.N., Zadymova, N.M., Pugachevich, P.P., Rabionovich, I.I. and Markina, Z.N.: Koll. Zh., 39 (1977) 513.
22. Papeschi, G., Bordi, S. and Costa, M.: Naa Chim., (1981) 407.
23. Markina, Z.N., Zadymova, N.M. and Bovkun, O.P.: Colloids and Surfaces, 22 (1987) 9.
24. Schramm, V.L. and Green, W.H.F.: Colloid Polymer Sci., 270 (1992) 694.
25. Ross, J.L., Bruce, W.D. and Janna, W.S.: Langmuir, 8 (1992) 2644.
26. Holcomb, C.D. and Zollweg, J.A.: J. Colloid Interface Sci., 154 (1992) 51.
27. Iliev, T.H. and Dushkin, C.D.: Colloid Polymer Sci., 270 (1992) 370.
28. Fainerman, V.B. and Lylyk, S.V.: Koll.Zh., 44 (1982) 598.
29. Fainerman, V.B.: Koll. Zh., 52 (1990) 921.
30. Fainerman, V.B.: Colloids and Surfaces, 62 (1992) 333.
31. Fainerman, V.B.: Koll. Zh., 41 (1979) 111.
32. Kazakov, V.N., Fainerman, V.B., Sinyachenko, O.V., Miller R., Joos, P., Lylyk, S.V., Ayko, A.E., Trukhin, D.V. and Ermolayeva, M.N.: Arch. Clin. Exp. Med. (Ukraine), 5 (1995) 3.
33. Joos, P. and Rillaerts, E.: J. Colloid Interface Sci. 79 (1981) 96.
34. Garrett, P.R. and Ward, D.R.: J. Colloid Interface Sci. 132 (1989) 475.
35. Fainerman, V.B., Makievski, A.V. and Joos, P.: Zh. Fiz. Khim., 67 (1993) 452.
36. MacLeod, C.A. and Radke, C.J.: J. Colloid Interface Sci., 160 (1993) 452.
37. MacLeod, C.A. and Radke, C.J.: J. Colloid Interface Sci., 166 (1994) 73.
38. Fainerman, V.B., Makievski, A.V. and Miller, R.: Colloids and Surfaces A, 75 (1993) 229.
39. Kao, R.L., Edwards, D.A., Wasan, D.T. and Chen, E.: J. Colloid Interface Sci., 148 (1993) 247.
40. Edwards, D.A., Kao, R.L. and Wasan, D.T.: J. Colloid Interface Sci. 155 (1993) 518.
41. Fainerman, V.B., Makievski, A.V.: Koll Zh. 54 (1992) 75.
42. Fainerman, V.B., Makievski, A.V.: Koll Zh. 54 (1992) 84.
43. Passerone, A., Liggieri, L., Rando, N., Ravera, F. and Ricci, E.: J. Colloid Interface Sci., 146 (1991) 152.
44. Liggieri, L., Ravera, F., Ricci, E. and Passerone, A.: Adv. Space Res. 11 (1991) 759.
45. Ravera, F., Liggieri, L. and Steinchen, A.: J. Colloid Interface Sci., 156 (1993) 109.
46. Miller, R., Sedev, R., Schano, K.-H., Ng, C. and Neumann, A.W.: Colloids and Surfaces, 69 (1993b) 209.
47. Horozov, T., Danov, K., Kralschewsky, P., Ivanov, I. and Borkwankar, R.: 1st World Congress on Emulsion, Paris, Vol. 2, (1993) 3-20-137.
48. Nagarajan, R. and Wasan, D.T.: J. Colloid Interface Sci., 159 (1993) 164.
49. Ilkovic, D.: Collec. Czechoslow. Commun., 6 (1934) 498.
50. Ilkovic, D.: J. Chim. Phys. Physicochem. Biol. 35 (1938) 129.
51. Pierson, F.W. and Whittaker, S.: J. Colloid Interface Sci., 52 (1976) 203.
52. Ward, A.F.H. and Tordai, L.: J. Phys. Chem. 74 (1946) 453.
53. Miller, R.: Colloid Polymer Sci. 258 (1980) 179.
54. Davies, J.T., Smith, J.A.C. and Humphreys, D.G.: Proc.Int. Conf. Surf. Act. Subst. 2 (1957) 281.
55. Miller, R. and Schano, K.-H.: Colloid Polymer Sci. 264 (1986) 277.
56. Miller, R. and Schano, K.-H.: Tenside Surfactants Detergents 27 (1990) 238.
57. Delahay, P. and Trachtenberg, I.: J. Amer. Chem. Soc., 79 (1957) 2355.
58. Delahay, P. and Fike, C.T.: J. Amer.Chem.Soc., 80 (1958) 2628.
59. Fainerman, V.B.: Zh.Fiz.Khim., 42 (1983) 457.
60. Fainerman, V.B., Makievski, A.V. and Miller, R.: Colloids and Surfaces A, 87 (1994) 61.
61. Fainerman, V.B., Makievski, A.V. and Joos, P.: Zh. Fiz. Khim., 67 (1993) 452.
62. Miller, R., Joos, P. and Fainerman, V.B.: Adv. Colloid Interface Sci. 49 (1994) 249.
63. Miller, R., Joos, P. and Fainerman, V.B.: Colloid Polymer Sci., 272 (1994) 731.
64. Miller, R., Hofmann, A., Schano, K.-H., Halbig, A. and Hartmann, R.: SÖFW-Journal, 118 (1992) 435.
65. Fainerman, V.B. and Miller, R.: Colloids and Surfaces A 97 (1995) 65.

### The authors of this paper

Dr. rer. nat. habil. Reinhard Miller studied mathematics at the University of Rostock and colloid science at the Technical University of Dresden. From 1973 to 1991 he worked at the Central Institute of Organic Chemistry of the Academy of Sciences in Berlin. In 1992 he joined the Max-Planck-Institute of Colloid and Surface Science in Berlin. His main interests are in the theory and experiments of surfactant transport, adsorption kinetics and interfacial rheology.

Dr. sc. nat. Valentin B. Fainerman studied chemical technology at Donetsk Technical University. Since 1970 he has worked at the Institute of Technical Ecology, Donetsk, Ukraine. The fields of scientific interest are thermodynamics of interfacial phenomena in multicomponent non-ideal and micellar systems; dynamic surface and interfacial tension, kinetics of adsorption, theoretical problems of chemical technology.

Dr. rer. nat. Karl-Heinz Schano was born in Landeck. He studied chemistry at the TH Leuna-Merseburg and colloid science at the Technical University Dresden. In his PhD thesis he worked in the field of phosphorous-organic compounds. Since 1976 he worked as a scientific coworker at the Central Institute of Organic Chemistry of the Academy of Sciences of the GDR. Main topic: characterisation of surfactant adsorption layers. (11704)



# Gesellschaft Deutscher Chemiker

## Fachgruppe Waschmittelchemie

### Mitgliederversammlung

Die Mitgliederversammlung der GDCh-Fachgruppe Waschmittelchemie fand am 29. April 1997 in Saarbrücken statt. Im Rahmen des Berichts des Vorstandes wurde vom Vorsitzenden der Fachgruppe, Dr. Chr. Grugel, insbesondere auf die Vorbereitung der Tagungen, die Wahlvorbereitung und die Unterstützung des Hauptausschusses Detergentien hingewiesen. Die Fachgruppentagung 1997 in Saarbrücken selbst wurde neben dem Tag der Tenside 1996 in Dresden vorbereitet.

Der Tag der Tenside 1996 war, wie bisher stärker physikalisch-chemisch und grundlagenorientiert, wissenschaftlich erfolgreich und soll deshalb 1998 wiederholt werden.

Weiter hat die Fachgruppe ein Symposium bei der Tagung der GDCh „Umwelt und Chemie“ im Oktober 1996 in Ulm durchgeführt. Auch hier wird sich die Fachgruppe aufgrund des Erfolges das nächste Mal – geplant Oktober 1998 – dann mit wahrscheinlich fünf anderen Fachgruppen der GDCh (Analytische Chemie, Anstrichstoffe und Pigmente, Umweltchemie und Ökotoxikologie, Makromolekulare Chemie, Wasserchemie) an einer erneuten Tagung „Umwelt und Chemie“ beteiligen.

Ferner betonte Dr. Grugel, daß die Beeinträchtigung der Umwelt durch Waschmittel auf ein Mindestmaß zurückgeführt werden konnte. Dies wird auch dadurch bestätigt, daß die Zusammensetzung der Waschmittel in Fachkreisen und in der Öffentlichkeit nicht mehr als herausragendes Umweltproblem gesehen wird. Insgesamt hat deshalb die Umweltpolitik bezüglich der Waschmittel keinen so hohen Stellenwert mehr. Einer der Gründe hierfür ist die Umstellung der Produkte durch die Waschmittelindustrie, u. a. auch hin zu den Konzentraten und Kompaktprodukten. Auch bessere Informationen für die Verbraucher haben zu einer sachgerechten Verwendung und damit insgesamt zu einer geringeren Umweltbelastung geführt. Die nicht unbedeutende Arbeit und Hilfe durch die GDCh-Fachgruppe Waschmittelchemie ist unbestritten.

Noch verbessert werden könnte nach Dr. Grugel die Einbeziehung der Kollegen aus den neuen Bundesländern in die gesamte Fachgruppenarbeit. Ein weiterer Punkt, der diskussions- und verbesserungswürdig ist, liegt zur Zeit in der Summe der Investitionen in Deutschland: Dr. Grugel betont, daß auch eine herausragende Wissenschaft nur einer entsprechend effizienten Wirtschaft folgt. Eine größere Akzeptanz nicht nur der Waschmittelchemie, sondern der Chemie insgesamt in einem Land, in dem keine großen Rohstoffe vorhanden sind, muß unbedingt erreicht werden.

### Hauptausschuß Detergentien

Über die Arbeit des Hauptausschusses Detergentien in den vergangenen Monaten berichtete Dr. Andree, Henkel KGaA:

Am 24. April 1997 fand in Frankfurt/M. ein Kolloquium mit 50 Teilnehmern statt, zu dem Referenten aus Industrie und Behörde zum Thema „Stand der Diskussion zur ökologischen Bewertung von Tensiden“ sprachen.

Der Hauptausschuß beschäftigte sich weiter mit folgenden Themen:

- Auswertung von Borgelalten von Wasserproben unterschiedlicher Herkunft in der Bundesrepublik
- Meinungsbildung zum Thema Duftstoffe in W- und R-Produkten (insbesondere endokrine Wirkung von Moschus-Derivaten)
- Kaskadenmodell: Etablierung der neuen und aussagekräftigen Methode als offizielle DIN-Methode zur Charakterisierung des Umweltverhaltens von Tensiden. Der geplante Ringversuch konnte nicht beginnen, da außerhalb der Industrie (CWH, BASF, Henkel) bisher keine Möglichkeiten bzw. finanziellen Mittel zur Verfügung standen.
- Bodenanalyse von kontaminierten Böden durch die Behandlung mit Tensiden, Entscheidung im Herbst 97 nach Präsentation des Themas.
- Analytik von Nonylphenolen in Probenarten der Umweltprobenbank der Bundesrepublik Deutschland, Ergebnis: Reduzierung auf 1/3. (Hintergrund: 1986 Selbstverzicht (z. B.

IKW, IPP) zur Verwendung von APEOs (Nonylphenol besitzt endokrine Wirksamkeit)).

Zukünftig: Übernahme von Themen aus dem Hauptausschuß Nährstoffe.

### Tagungen und Veranstaltungen der Fachgruppe

Der 30. und 31. März 1998 ist für den Tag der Tenside in Leipzig vorgesehen. Die wissenschaftliche Verantwortung für die Vorbereitung von der Seite der Fachgruppe hat Prof. Hauthal übernommen. Einer der Schwerpunkte wird die Analytik sein. Die vom Vorstand beschlossene Mitwirkung der Deutschen Bunsen-Gesellschaft für Physikalische Chemie geschieht über Prof. H. Hoffmann, Bayreuth.

Im Oktober 1998 ist diesmal in Karlsruhe das Treffen „Umwelt und Chemie“ geplant, die Fachgruppe Waschmittelchemie wird ihre Beiträge in die Gesamtagung integrieren. Die nächste Fachgruppentagung ist im Jahr 1999 in der ersten Maiwoche in Lüneburg geplant. Die Mitgliederversammlung begrüßt den Vorschlag des Vorstandes einstimmig.

### Wahl des Vorstandes

Unter der Wahlleitung von Dr. Behret wird der Vorstand per Akklamation gewählt. Der neue Vorstand in der Zusammensetzung

Dr. H. Andree	Henkel KGaA, Düsseldorf
Dr. G. Becker	Lever GmbH, Hamburg
Dr. U. Buller	Fraunhofer-Gesellschaft, München
Dr. H. U. Jäger	BASF AG, Ludwigshafen
Dr. P. Jürges	Hoechst AG, Frankfurt
Dr. L. Nitschke	Bayerische Landesanstalt für Wasserforschung, München
Prof. Dr. H. Rehage	Universität/ Gesamthochschule Essen
Dr. W. Ruback	Hüls AG, Marl
Dr. D. Schermer	Procter & Gamble GmbH, Schwalbach am Taunus

tritt sein Amt zum 1. Januar 1998 für die vierjährige Amtsperiode an. Entsprechend der Satzung der GDCh werden in einer ersten Sitzung der Vorsitzende und die beiden Stellvertreter bestimmt. (60624)